Characterization of a new 4.5 kV Press Pack SPT+ IGBT for Medium Voltage Converters

Rodrigo Alvarez
Power Electronics Group
Technische Universitaet Dresden,
Dresden, Germany
Rodrigo.alvarez@mailbox.tu-dresden.de

Felipe Filsecker
Power Electronics Group
Technische Universitaet Dresden,
Dresden, Germany
Felipe.filsecker@mailbox.tu-dresden.de

Steffen Bernet
Power Electronics Group
Technische Universitaet Dresden,
Dresden, Germany
Steffen.bernet@tu-dresden.de

***Abstract*—Recently developed IGBT press pack devices have become a competition for IGCTs in high power industrial applications. This paper presents an overview of state-of-the-art medium voltage power semiconductors with active turn-off capability. A new 85 mm, 4.5 kV, 1.2 kA press pack SPT+ IGBT and the corresponding freewheeling diode are characterized at hard switching as a function of the parameters dc-link voltage, load current, junction temperature, stray inductance and gate unit conditions.**

I. Introduction

Recent technology developments of 3.3 kV, 4.5 kV and 6.5 kV IGBTs and IGCTs enabled a substantial improvement of medium voltage converters during the last years [1]–[3]. While medium voltage IGBT modules clearly dominate in traction converters, IGCT press pack devices are mainly used in high power industrial applications, due to advantageous features of press pack cases compared to modules, like a higher thermal and power cycling capability and an explosion-free failure mode [4], [5].

However, recently developed press pack IGBT devices combine the advantages of IGBTs with those of press pack cases. Thus, press pack IGBTs have become a competition for IGCTs in medium and high power industrial applications like medium voltage drives (MVD) for rolling mills, marine, mining, chemistry, oil and gas. New medium voltage converters require power semiconductors featuring a high blocking voltage as well as low conduction and switching losses. While the basic IGCT wafer design does not enable substantial improvements, several innovations, such as the Field Stop (FS) technology, the Injection-Enhanced Gate Transistor (IEGT) and the Soft Punch Through (SPT and SPT+) technology, have been introduced for the IGBT in the recent years. Several authors have compared IGBTs on the basis of the afore mentioned technologies for hard and soft switching [6]–[9]. The SPT+ technologies realize low losses, soft switching waveforms, a switching-self-clamping-mode and wide SOA limits [8], [9].

The new Westcode SPT+ IGBT press pack combines the advantages of the SPT+ IGBT technology with the advantages of press pack housing. The goal of this paper is a detailed characterization of the new 85 mm (4.5 kV, 1.2 kA) Westcode SPT+ IGBT press pack at hard switching. Both IGBT and the corresponding freewheeling diode are characterized at hard turn-on and turn-off transients.

II. Overview of MV power semiconductors and drives

Maximum nominal voltage and current ratings of available power semiconductors with turn-off capability are shown in Fig. 1. Both commercially available IGBT modules and asymmetrical IGCTs achieve maximum device voltages of 6.5 kV. So far press pack IGBTs feature maximum device blocking voltages of 4.5 kV. It is interesting to note that the maximum turn-off current of the 125 mm (4.5 kV, 2.4 kA) press pack IGBT ($I_{C,M}$ = 4.8 kA) is slightly lower than that of the largest currently available 91 mm 4.5 kV IGCT (I_{TGQM}=5.5 kA). However, compared to the IGCT, the press pack IGBT features several advantages, like short circuit current limitation, short circuit turn-off capability, an adjustment of the switching behavior by the gate unit and a simpler device parallel and series connection, which simplify the converter design substantially [1]. Table I shows the voltage and power ranges of state-of-the-art industrial medium voltage converters for drives. Both IGBTs and IGCTs have replaced GTOs almost completely in the last years. The Three Level Neutral Point Clamped-Voltage Source Converter (3L NPC-VSC), the Multi Level Series Connected H Bridge-Voltage Source Converter (ML SCHB-VSC), also known as Robicon topology, and the Five Level H Bridge-Voltage Source Converter (5L HB-VSC), consisting of an H-bridge of two 3L NPC phase legs per phase are commonly applied topologies. Recently 4.5 kV press pack IGBT devices have become a competition to 4.5 kV IGCTs in the widely distributed 3.3 kV 3L NPC-VSCs, as well as 6.6 kV 5L HB-VSCs.

III. Semiconductor Data and Test-bench

The 85 mm 4.5 kV press pack IGBT T1200EB45E (Westcode), the commercially available gate unit C0030BG400 (Westcode) and the widely distributed 68 mm 4.5 kV press pack diode D1031SH45T (Infineon) have been selected for the characterization of the devices at hard switching. Characteristic values of the power semiconductors and the gate unit are summarized in Table II.

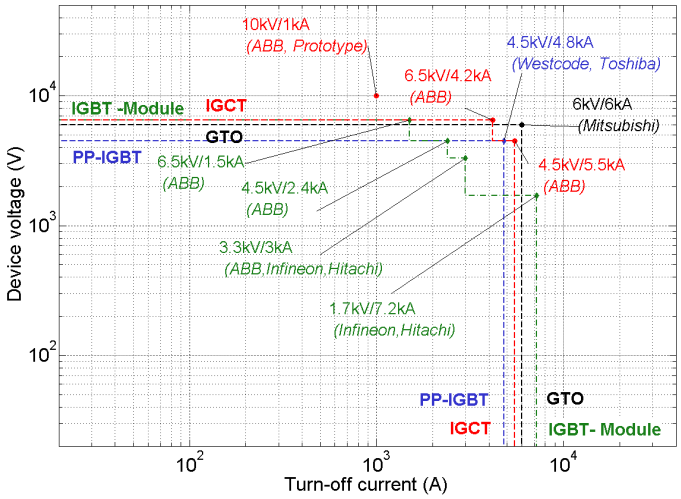

Fig. 1: Blocking voltage and maximum turn-off currents of state-of-the-art IGBTs and asymmetrical IGCTs. Date: June 2009

TABLE I: Maximum power ratings of single unit Medium Voltage Converters

Semi-conductor	Package	Voltage [kV]	Power [MVA]	Topology
IGBT	Module	2.3 - 6.6	10	3L NPC-VSC
IGBT	Module	2.3 - 13.8	35	ML SCHB-VSC
IGBT	Press pack	3.3	10	3L NPC-VSC
IGBT	Press pack	6.6	20	5L HB-VSC
IGCT	Press pack	2.3 - 4.16	10	3L NPC-VSC
IGCT	Press pack	4.16 - 6.9	24	5L SCHB-VSC

A buck converter was chosen as test circuit configuration for the investigation of the devices at hard switching, see Figs. 2 and 3 [10]. To enable an accurate adjustment of the stray inductance despite a large dc-link capacitor bank C_{DC} (4.5 mF), the dc-link voltage is supported by a clamp capacitor C_{Cl} (220 µF) close to the stack. A robust mechanical design was realized by 2 mm thick copper plates as connections between the dc-link capacitor C_{DC}, the clamp capacitor C_{Cl} and the stack. Thus the mechanical construction of the test bench is able to withstand short circuit currents of about 200 kA in case of a device failure. The two diodes (D_{r1}, D_{r2}) and the fuse F are important components of the protection concept. The fuse avoids the complete discharge of the dc-link capacitors through the stack, and the diodes D_{r1}, D_{r2} limit possible negative voltages across the dc-link capacitor preventing an oscillation of the failure short circuit current. The double pulse operation of the buck converter is the reason therefore, that the device junction temperatures can be adjusted by two heaters, which control the case temperatures [10]. The dc-link capacitor is charged by a high voltage power supply before the start of the measurements. The variation of several measurement parameters, as depicted in Table III, generate about 500 measurements to characterize

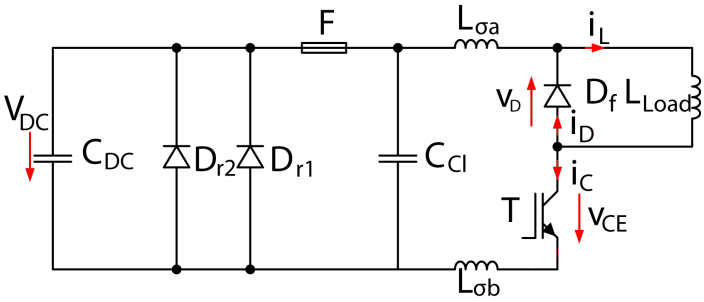

Fig. 2: Test circuit (C_{DC} = 4.5 mF, C_{Cl} = 220 µF, $L_{\sigma a}$+ $L_{\sigma b}$ = 120 . . . 210 nH, L_{Load} = 1 mH)

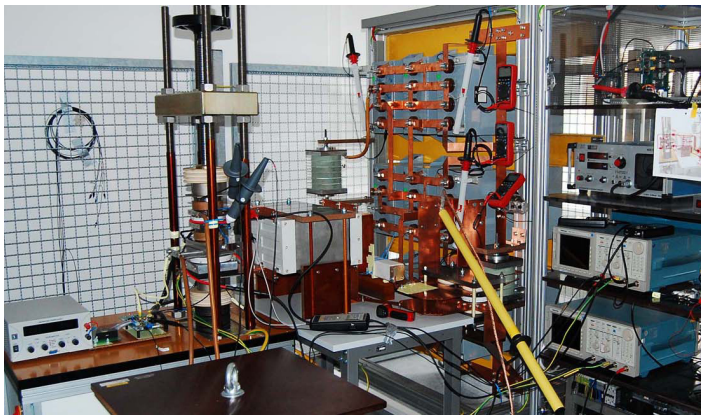

Fig. 3: IGBT press pack test bench

the switching behavior of IGBT and diode. Thus, a partially automated measurement system was used. The values of V_{DC} and i_L are set through a LabVIEW graphical user interface in a computer connected to the test bench by fiber optic cable. The results are captured by two 8-bit four-channel digital oscilloscopes (Tektronix TDS714L), capable of working at 500 MS/s sample rate. The storage and analysis of the data is carried out on a PC.

TABLE II: Data of PP-IGBT, diode and gate unit

PP-IGBT Westcode T1200EB45E		**PP-Diode Infineon D1031SH45T**		**Gate Unit Westcode C0030BG400**	
V_{CES}	4500 V	V_{RRM}	4500 V	$V_{G,on/off}$	±15 V
$V_{DC\text{-}link}$	2800 V	I_{FRMSM}	2300 A	$R_{G,on}$	3.3 . . . 6.8 Ω
$I_{C(DC)}$	2132 A	I_{FAVM}	1470 A	$R_{G,off}$	2.2 . . . 6.8 Ω
$I_{C(nom)}$	1200 A	I_{RRM}	1500 A	P_o	12 W

IV. Experimental Results

This section presents an overview of the results and analysis based on the experimental results obtained with the previously described testbench for diverse parameter sets, see Table III. The circuit of the main components of the experimental set-up is shown in Fig. 2. Three gate unit configurations have been defined:

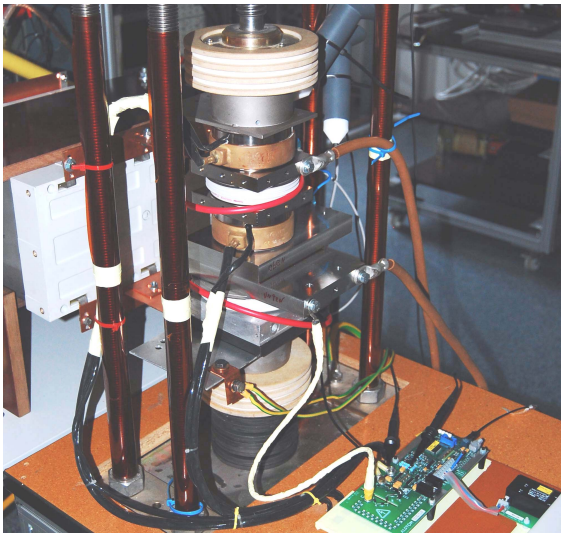

Fig. 4: IGBT Stack

TABLE III: Data of test-bench and parameter variations

C_{DC}	4.5 mF
C_{Cl}	220 µF
L_{Load}	1 mH
V_{DC}	2, 2.5 kV
i_L	100…1800 A
L_σ	120, 210 nH
T_j	25, 60, 90, 125 °C
$R_{G,on}$	3.3, 5.6 and 6.8 Ω
$R_{G,off}$	2.2, 3.6 and 6.8 Ω

- Gate unit 1 (GU-1) with $R_{G,on}$ = 3.3, $R_{G,off}$ = 2.2 Ω
- Gate unit 2 (GU-2) with $R_{G,on}$ = 5.6, $R_{G,off}$ = 3.6 Ω
- Gate unit 3 (GU-3) with $R_{G,on}$ = 6.8, $R_{G,off}$ = 6.8 Ω

The stray inductance can be adjusted to values of $L_{\sigma 1} = 120\,\text{nH}$ and $L_{\sigma 2} = 210\,\text{nH}$ to investigate the influence of this crucial parameter for the converter and stack design.

For every set of temperature, dc-link voltage, gate unit and stray inductance, the switching behavior of IGBT and diode is investigated for seven different collector currents. Figs. 5 and 6 show exemplarily measurements of the IGBT and diode switching behavior at $T\text{j} = 90\,°\text{C}$, 2.5 kV dc-link, GU-1 and $L_{\sigma 1} = 120\,\text{nH}$.

A. Parameter Definitions

The following variables have been used to analyze the switching behavior of IGBT and diode:

- V_{DC}, I_L : DC voltage and load current (constant during the commutation)
- $I_{C,max}$: Maximum IGBT current value during the natural commutation
- $V_{CE,max}$: Maximum IGBT voltage value during forced commutations
- I_{rrm} : Peak reverse recovery current

Definitions of device voltages and currents to calculate rates of change are shown in Figs. 7, Fig. 8 and Table IV.

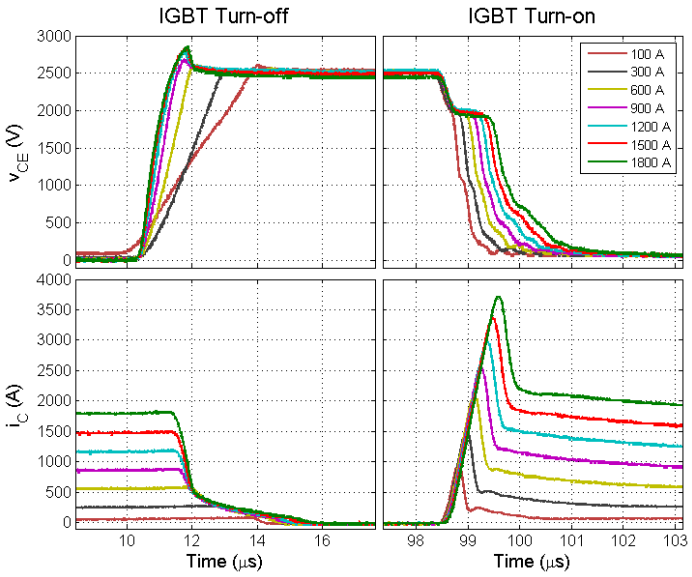

Fig. 5: IGBT switching waveforms for different collector currents for one set of parameters ($T\text{j} = 90\,°\text{C}$, $V_{DC} = 2.5\,\text{kV}$, $L_{\sigma 1} = 120\,\text{nH}$ and GU-1).

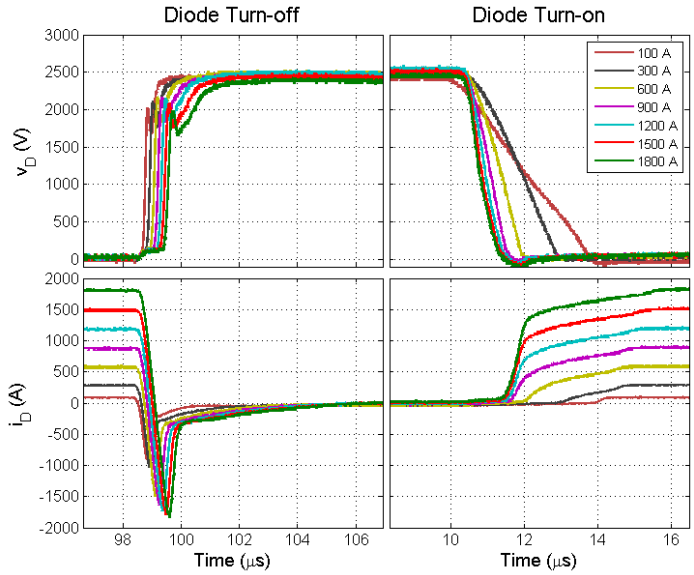

Fig. 6: Diode switching waveforms for different collector currents for one set of parameters ($T\text{j} = 90\,°\text{C}$, $V_{DC} = 2.5\,\text{kV}$, $L_{\sigma 1} = 120\,\text{nH}$ and GU-1).

The voltage and current slopes are defined as follows:

$$\frac{\mathrm{d}i}{\mathrm{d}t} = \left| \frac{i_2 - i_1}{t(i_2) - t(i_1)} \right| \tag{1}$$

$$\frac{\mathrm{d}v}{\mathrm{d}t} = \left| \frac{v_2 - v_1}{t(v_2) - t(v_1)} \right| \tag{2}$$

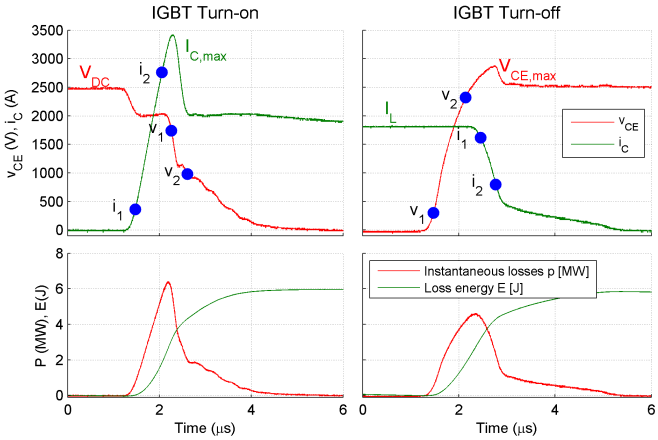

Fig. 7: Definitions of IGBT voltages and currents for calculations of dv/dt and di/dt, switching losses (Tj = 90 °C, $V_{\mathrm{DC}} = 2.5\,\mathrm{kV}$, $i_{\mathrm{C}} = 1.8\,\mathrm{kA}$, $L_{\sigma 1} = 120\,\mathrm{nH}$ and GU-1).

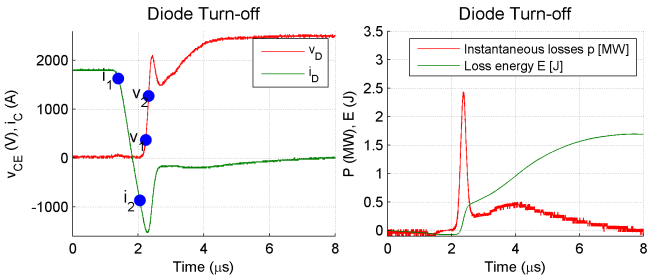

Fig. 8: Definitions of diode voltages and currents for calculations of dv/dt and di/dt, switching losses, (Tj = 90 °C, $V_{\mathrm{DC}} = 2.5\,\mathrm{kV}$, $i_{\mathrm{C}} = 1.8\,\mathrm{kA}$, $L_{\sigma 1} = 120\,\mathrm{nH}$ and GU-1).

TABLE IV: Definition of points for dx/dt calculations

		v_1	v_2	i_1	i_2
IGBT	on	$0.7V_{\mathrm{DC}}$	$0.4V_{\mathrm{DC}}$	$0.1I_{\mathrm{C,max}}$	$0.8I_{\mathrm{C,max}}$
	off	$0.1V_{\mathrm{DC}}$	$0.8V_{\mathrm{DC}}$	$0.9I_{\mathrm{L}}$	$0.45I_{\mathrm{L}}$
Diode	off	$0.15V_{\mathrm{DC}}$	$0.5V_{\mathrm{DC}}$	$0.9I_{\mathrm{L}}$ $+0.1I_{\mathrm{rrm}}$	$0.8I_{\mathrm{rrm}}$ $+0.2I_{\mathrm{L}}$

B. Influence of Gate Units

Both IGBT and diode switching waveforms depend on the gate unit conditions. IGBT turn-on transients with GU-1 and GU-3 are depicted in Fig. 9 for one operating point. Obviously the larger gate resistance of GU-3 substantially decreases the rate of current rise and voltage fall. Fig. 10 shows, that the di_{C}/dt changes from 4 kA/μs for GU-1 to 2 kA/μs for GU-3 at the nominal current i_{C}. The same effect can also be observed for the dv_{CE}/dt , which changes from 3 kV/μs for GU-1 to 1 kV/μs for GU-3. Figs. 11 and 12 show the corresponding waveforms and slopes for the freewheeling diode turn-off. As expected a larger gate resistance decreases the di_{D}/dt, the peak reverse recovery current I_{rrm} and the dv_{D}/dt. Even at the smallest gate resistance of $R_{\mathrm{G,on}} = 3.3\,\Omega$ the moderate di_{D}/dt causes a soft turn-off behavior of the diode and moderate I_{rrm} values. A

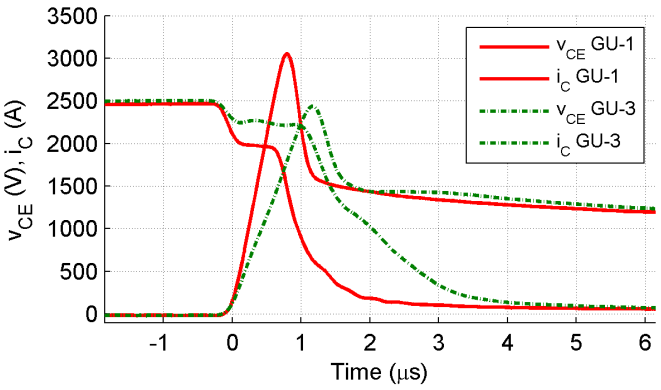

Fig. 9: IGBT turn-on transients at different gate unit conditions (Tj = 125 °C, $V_{\mathrm{DC}} = 2.5\,\mathrm{kV}$, $i_{\mathrm{C}} = 1.2\,\mathrm{kA}$, $L_{\sigma 1} = 120\,\mathrm{nH}$).

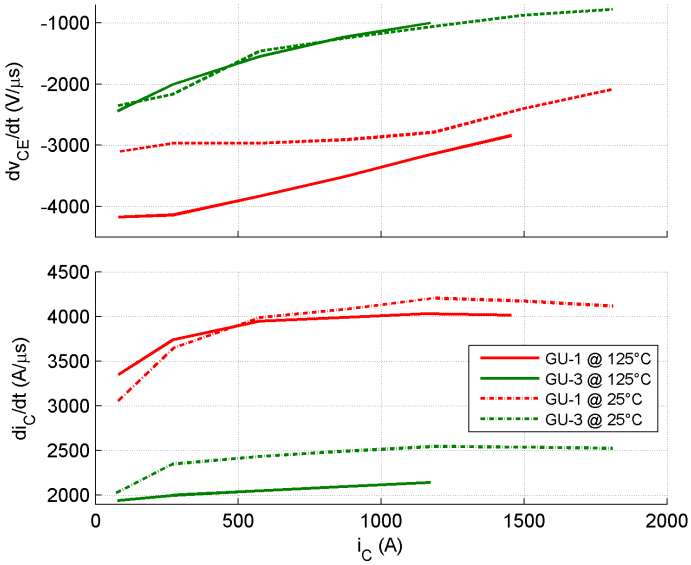

Fig. 10: IGBT turn-on di_{C}/dt and dv_{CE}/dt at different gate unit conditions (Tj = 25 and 125 °C, $V_{\mathrm{DC}} = 2.5\,\mathrm{kV}$, $L_{\sigma 1} = 120\,\mathrm{nH}$).

snappy behavior of the diode has not been observed in the entire operating range. In contrast to the IGBT turn-on behavior, the IGBT turn-off transients only slightly change for varying gate unit configurations, see Figs. 13 and 14.

C. Influence of Stray Inductance

This section presents the effects of different stray inductances L_σ on the IGBT and diode switching behavior, see Figs. 15 to 20.

Obviously the different stray inductances L_σ do not change the rates of current slopes during IGBT turn-on and turn-off transients substantially (Figs. 16, 18 and 20). In contrast the larger stray inductance $L_{\sigma 2} = 210\,\mathrm{nH}$ leads to a reduced voltage v_{CE} during the current rise at IGBT turn-on transients (Fig. 16) and higher device overvoltages during falling currents at the IGBT and diode turn-off transients (Figs. 18 and 20). As a result, an increase of the stray inductance from $L_{\sigma 1} = 120\,\mathrm{nH}$

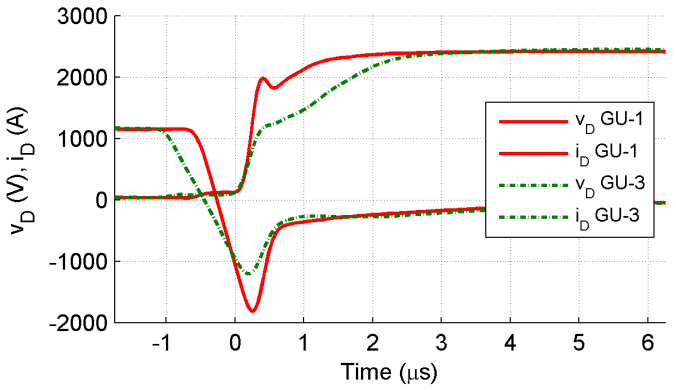

Fig. 11: Diode Turn-off transients at different gate unit conditions ($Tj = 125\,°C$, $V_{DC} = 2.5\,kV$, $i_C = 1.2\,kA$, $L_{\sigma 1} = 120\,nH$).

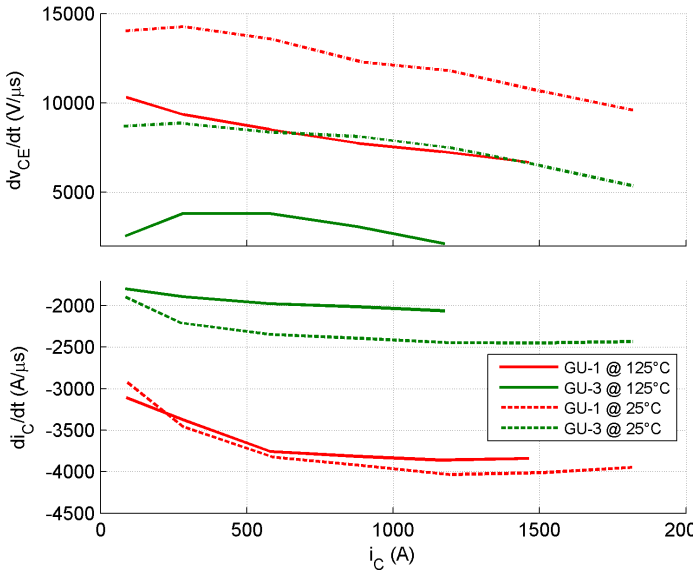

Fig. 12: Diode Turn-off $\mathrm{d}i_D/\mathrm{d}t$ and $\mathrm{d}v_D/\mathrm{d}t$ at different gate unit conditions ($Tj = 25$ and $125\,°C$, $V_{DC} = 2.5\,kV$, $L_{\sigma 1} = 120\,nH$).

to $L_{\sigma 2} = 210\,nH$ reduces the IGBT turn-on losses by around $20\ldots40\,\%$ ($2\ldots2.3\,J$) for GU-3 and GU-1 respectively, see Fig. 15. For the IGBT turn-off behavior an increase of the stray inductance causes a proportional increase of the overvoltage, having almost no impact on the $\mathrm{d}i_C/\mathrm{d}t$, $\mathrm{d}v_{CE}/\mathrm{d}t$ or the IGBT turn-off losses, see Fig. 17. The diode turn-off transient shows almost no change of the peak reverse recovery current I_{rrm}. However, the increase of the stray inductance and the increased diode overvoltage leads to an increase of the diode turn-off losses by about $10\ldots17\,\%$ ($0.2\ldots0.5\,J$) for GU-3 or GU-1 respectively, see Fig. 19.

The total switching losses of IGBT and diode are reduced as a result of the larger stray inductance (Fig. 21). This is caused by the significant reduction of the IGBT turn-on losses, which overcompensate the increased diode turn-off losses (Fig. 21).

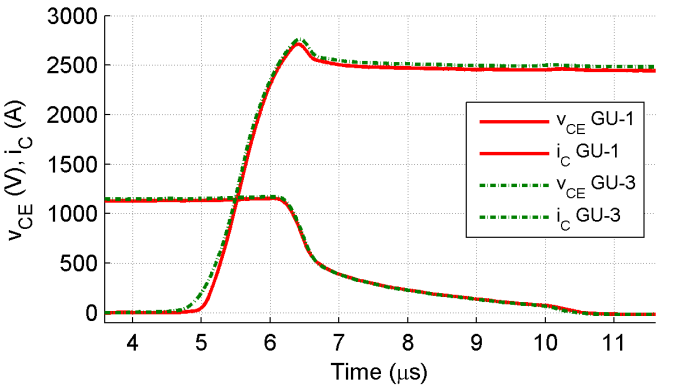

Fig. 13: IGBT turn-off transients at different gate unit conditions ($Tj = 125\,°C$, $V_{DC} = 2.5\,kV$, $i_C = 1.2\,kA$, $L_{\sigma 1} = 120\,nH$).

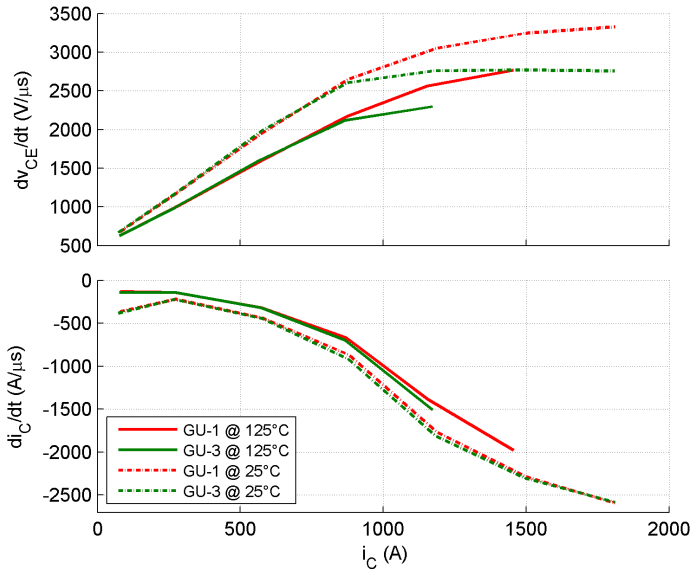

Fig. 14: IGBT turn-off $\mathrm{d}i_C/\mathrm{d}t$ and $\mathrm{d}v_{CE}/\mathrm{d}t$ at different gate unit conditions ($Tj = 25$ and $125\,°C$, $V_{DC} = 2.5\,kV$, $L_{\sigma 1} = 120\,nH$).

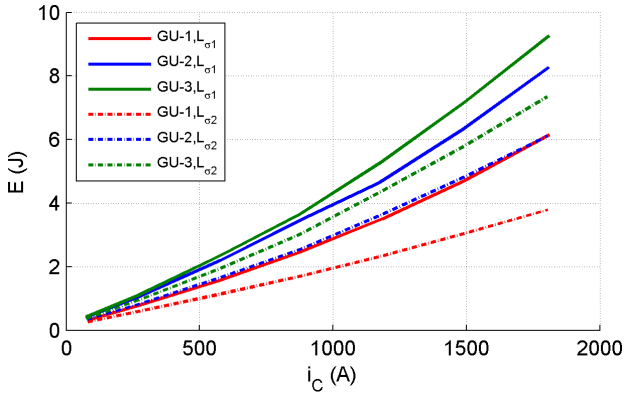

Fig. 15: IGBT turn-on Losses at different stray inductances L_σ ($Tj = 25\,°C$, $V_{DC} = 2.5\,kV$).

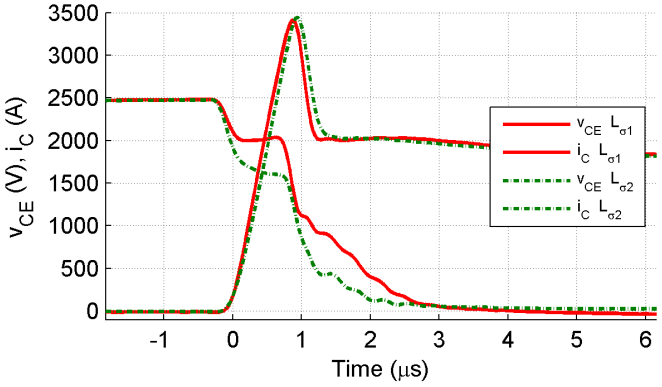

Fig. 16: IGBT turn-on transients at different stray inductances L_σ ($Tj = 25\,°C$, $V_{DC} = 2.5\,kV$, $i_C = 1.8\,kA$ and GU-1).

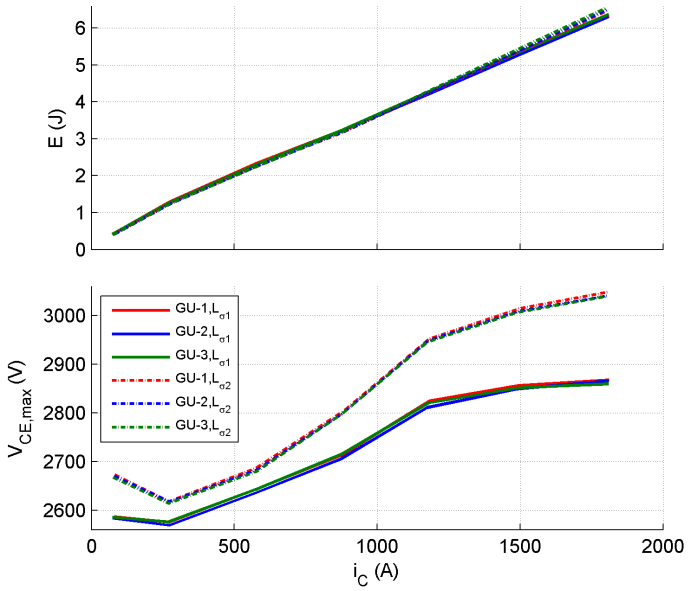

Fig. 17: IGBT turn-off Losses at different stray inductances L_σ ($Tj = 25\,°C$, $V_{DC} = 2.5\,kV$).

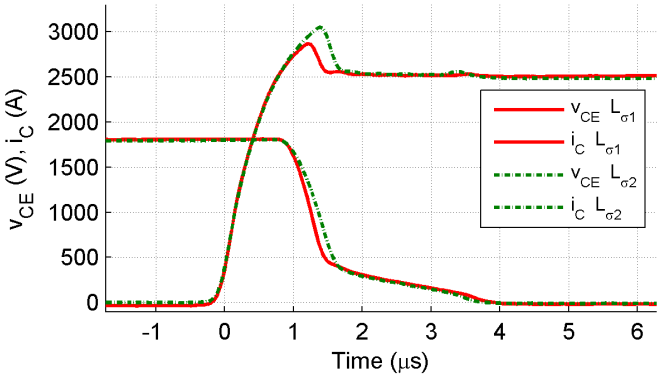

Fig. 18: IGBT turn-off transients at different stray inductances L_σ ($Tj = 25\,°C$, $V_{DC} = 2.5\,kV$, $i_C = 1.8\,kA$ and GU-1).

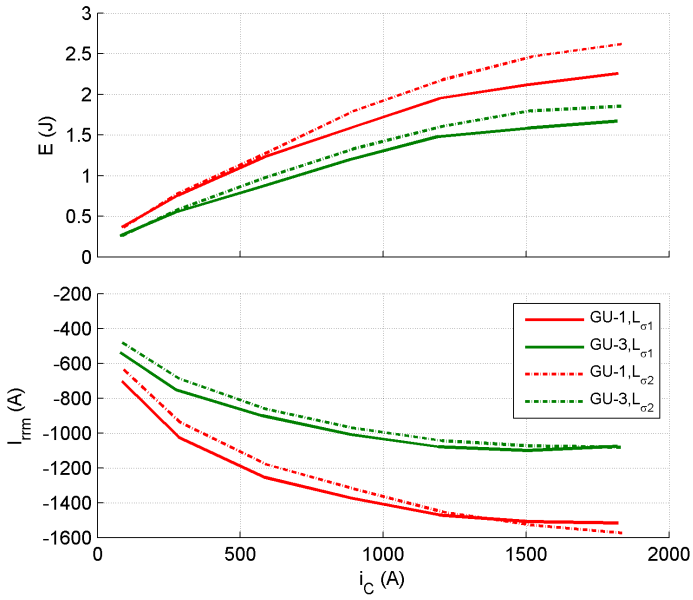

Fig. 19: Diode Turn-off Losses and reverse recovery current at different stray inductances L_σ ($Tj = 25\,°C$, $V_{DC} = 2.5\,kV$).

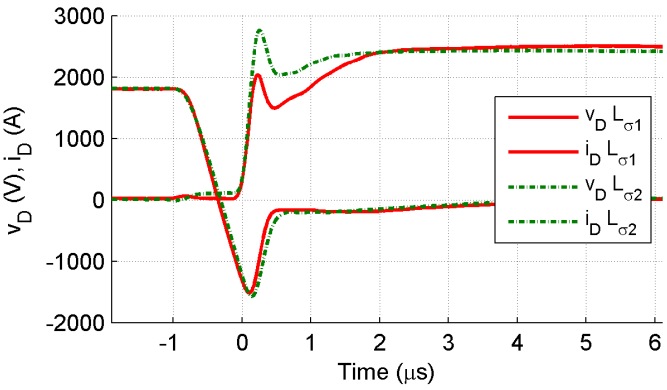

Fig. 20: Diode Turn-off waveforms at different stray inductances L_σ ($Tj = 25\,°C$, $V_{DC} = 2.5\,kV$, $i_C = 1.8\,kA$ and GU-1).

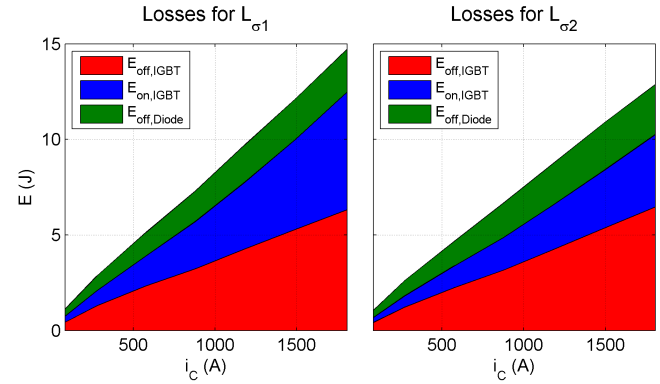

Fig. 21: Loss distribution for L_σ variations as a function of collector current i_C ($Tj = 25\,°C$, $V_{DC} = 2.5\,kV$ and GU-1).

Due to the moderate $\mathrm{d}i_\mathrm{C}/\mathrm{d}t$ at turn-on and turn-off transients even at the smallest gate resistances both IGBT and diode are not stressed with high overvoltage values during stationary operation at $L_{\sigma 2} = 210\,\mathrm{nH}$. However, the final choice of the stray inductance (L_σ) also depends on the mechanical design of the converter, the occurring maximum dc voltages, as well as the principle and design of the short circuit protection scheme of the IGBT gate unit.

D. Switching Losses

The temperature dependence of the losses is shown in Figs 22 ... 25.

The total switching losses of IGBT and diode are defined in (3).

$$E_\mathrm{Total} = E_\mathrm{on,IGBT} + E_\mathrm{off,IGBT} + E_\mathrm{off,Diode} \tag{3}$$

with

- $E_\mathrm{on,IGBT}$: IGBT turn-on switching losses
- $E_\mathrm{off,IGBT}$: IGBT turn-off switching losses
- $E_\mathrm{off,Diode}$: Diode turn-off switching losses

The total losses for the gate unit set-up (GU-1) with the smallest gate unit resistances at $V_\mathrm{DC} = 2.5\,\mathrm{kV}$ can be seen in Fig. 22. Obviously the total losses almost linearly increase with the rising collector current.

The total losses for the nominal current $i_\mathrm{C} = 1.2\,\mathrm{kA}$ increase by about 22 % from 25 °C to 125 °C (9.7 J to 11.9 J). The IGBT turn-off losses, turn-on losses and the diode turn-off losses are shown in Figs. 23 to 25 for $V_\mathrm{DC} = 2.5\,\mathrm{kV}$ and GU-1.

The IGBT turn-off losses increase almost linear with the rising collector current between 3.58 mJ/A at 25 °C and 4.23 mJ/A at 125 °C. The losses at the nominal current $i_\mathrm{C} = 1.2\,\mathrm{kA}$ increase by about 14 % from 25 °C to 125 °C (4.3 J to 4.9 J) for the GU-1 set up, see Fig. 23.

The IGBT turn-on losses depend linearly on the collector current between between 3.15 mJ/A at 25 °C and 3.34 mJ/A at 125 °C (Fig. 24). The turn-on losses at the nominal current $i_\mathrm{C} = 1.2\,\mathrm{kA}$ rise by about 11 % from 25 °C to 125 °C (3.56 J to 3.96 J).

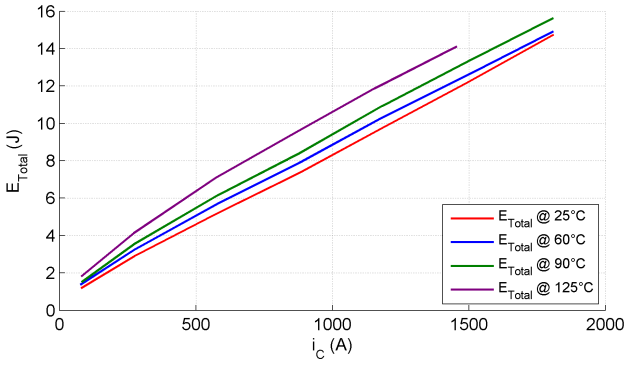

Fig. 22: Total switching losses as function of collector current i_C with $T\mathrm{j}$ as parameter ($V_\mathrm{DC} = 2.5\,\mathrm{kV}$, $L_{\sigma 1} = 120\,\mathrm{nH}$ and GU-1).

The function of diode turn-off losses and device current is non linear. At the nominal current $i_\mathrm{C} = 1.2\,\mathrm{kA}$ the diode turn-off losses increase by about 63 % from 25 °C to 125 °C (1.95 J to 3.17 J). If the losses are linearized the slope of the loss functions is in a range between 1.47 mJ/A at 25 °C and 2.78 mJ/A at 125 °C.

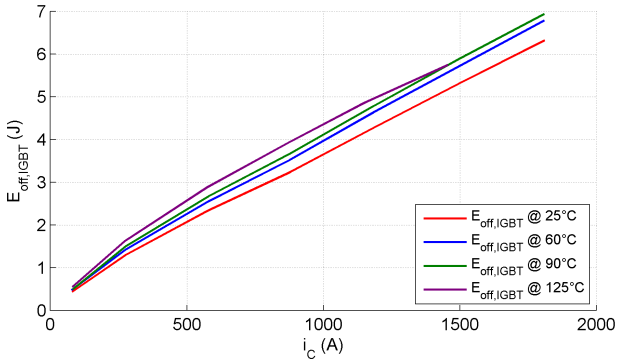

Fig. 23: IGBT Turn-off losses as function of collector current i_C with $T\mathrm{j}$ as parameter ($V_\mathrm{DC} = 2.5\,\mathrm{kV}$, $L_{\sigma 1} = 120\,\mathrm{nH}$ and GU-1).

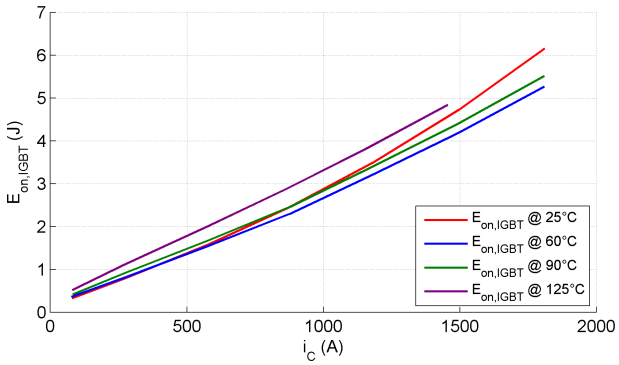

Fig. 24: IGBT Turn-on losses as function of collector current i_C with $T\mathrm{j}$ as parameter ($V_\mathrm{DC} = 2.5\,\mathrm{kV}$, $L_{\sigma 1} = 120\,\mathrm{nH}$ and GU-1).

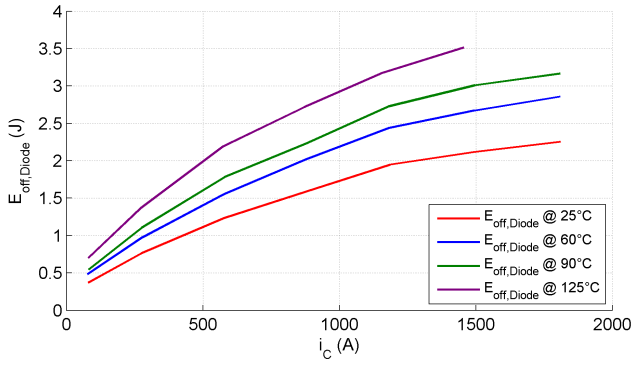

Fig. 25: Diode Turn-off losses as function of collector current i_C with $T\mathrm{j}$ as parameter ($V_\mathrm{DC} = 2.5\,\mathrm{kV}$, $L_{\sigma 1} = 120\,\mathrm{nH}$ and GU-1).

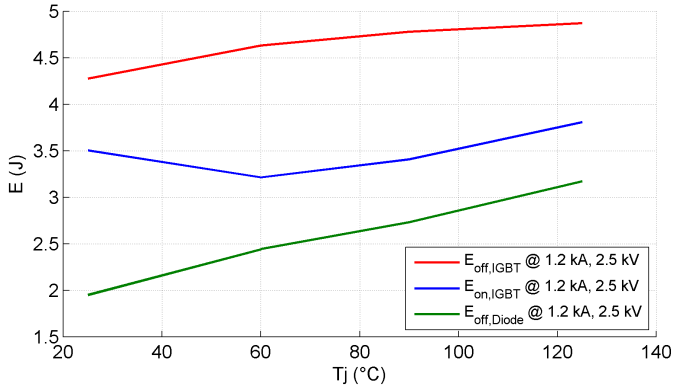

Fig. 26: Switching losses as function of junction temperature Tj ($V_{DC} = 2.5\,kV$, $i_C = 1.2\,kA$, $L_{\sigma 1} = 120\,nH$ and GU-1).

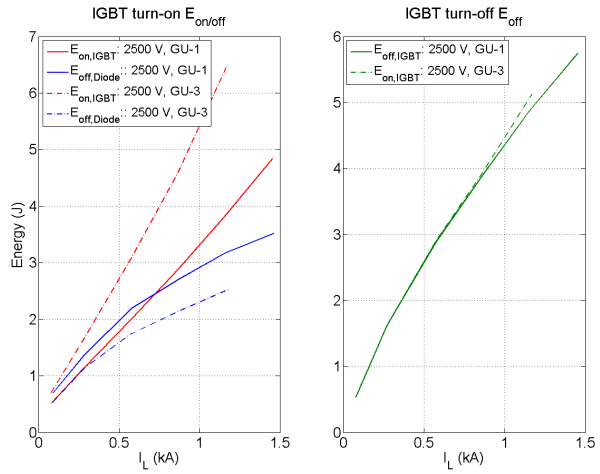

Fig. 27: Losses as function of i_C current for GU-1 and GU-3 ($Tj = 125\,°C$, $V_{DC} = 2.5\,kV$ and $L_{\sigma 1} = 120\,nH$).

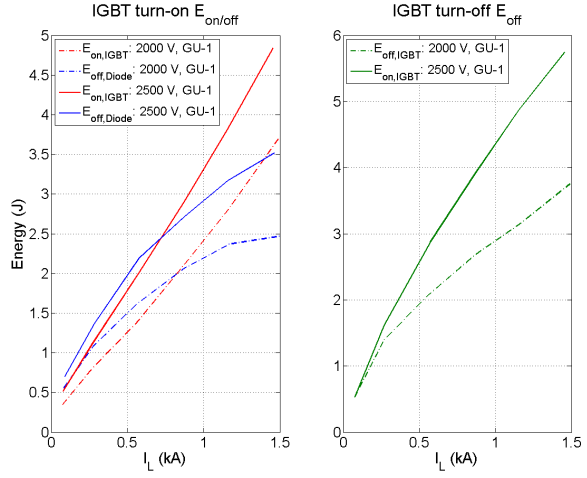

Fig. 28: IGBT and diode energy losses, $V_{DC} = 2\,kV$ and $V_{DC} = 2.5\,kV$ ($Tj = 125\,°C$, $L_{\sigma 1} = 120\,nH$ and GU-1).

The IGBT and diode switching losses as a function of the junction temperature can be taken from Fig. 26. While IGBT turn-off and diode turn-off losses almost linearly increase with the junction temperature the IGBT turn-on losses slightly fall from $Tj = 25\,°C$ to $Tj = 60\,°C$.

The influence of the gate unit set-up on the switching losses is depicted in Fig. 27. It should be noted, that the applied original Westcode gate unit is not capable of switching larger currents than 1.5 kA for $Tj = 125\,°C$. For larger currents, the short circuit turn-off mechanism of the gate unit is activated at IGBT turn-on transients. As mentioned before the gate unit set-up has a negligible influence on the IGBT turn-off losses. In contrast, the gate unit conditions strongly influence the IGBT turn-on and diode turn-off losses ($E_{on,IGBT}$ increases about 63.5 % for GU-3 and $E_{off,Diode}$ increases about 28 % for GU-3 at $i_C = 1.2\,kA$).

Fig. 28 shows the function of the switching losses for dc-link voltages of $V_{DC} = 2\,kV$ and $V_{DC} = 2.5\,kV$.

E. Trajectories and Maximum Instantaneous Power

Unfortunately the IGBT manufacturer has not yet provided a data sheet or a Safe Operating Area for the new press pack IGBT (T1200EB45E). During the conducted research of this paper, IGBT and diode have been tested for the conditions shown in Table III. The semiconductors being investigated feature a good switching behaviour in all investigated operating points. Exemplarily IGBT and diode switching waveforms and trajectories at $V_{DC} = 2.5\,kV$, the current of $i_C = 1.5\,kA$, $Tj = 125\,°C$, $L_{\sigma 1} = 120\,nH$ and the lowest recommended gate resistances (GU-1) can be taken from Figs. 29 to 31. In this operating point maximum instantaneous powers of $p_{max} = 6.08\,MW$ (IGBT turn-on transient), $p_{max} = 3.56\,MW$(IGBT turn-off transient) and $p_{max} = 2.81\,MW$ (diode turn-on transient) have been determined.

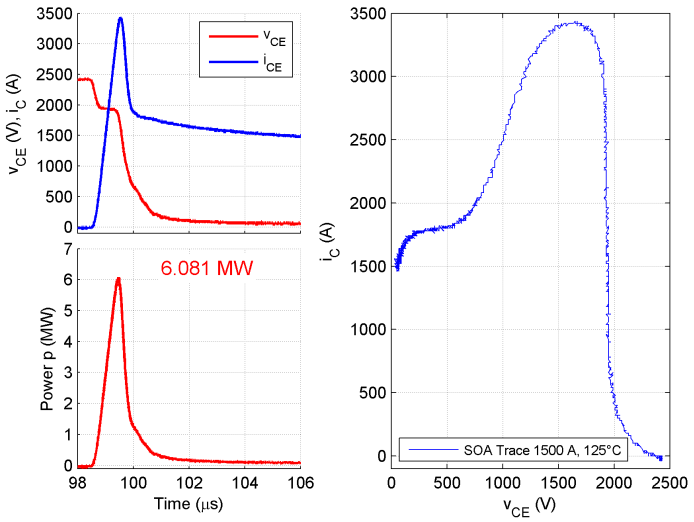

Fig. 29: IGBT turn-on waveforms, power and SOAR ($Tj = 125\,°C$, $V_{DC} = 2.5\,kV$, $i_C = 1.5\,kA$, $L_{\sigma 1} = 120\,nH$ and GU-1).

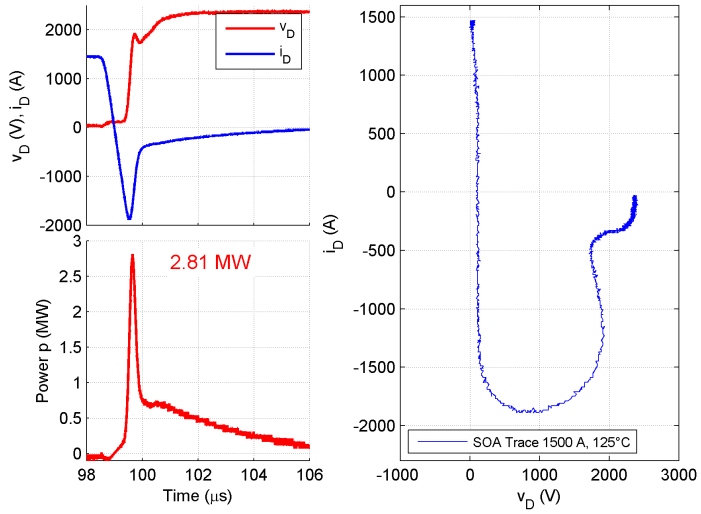

Fig. 30: Diode turn-off waveforms, power and SOAR (Tj = 125 °C, V_{DC} = 2.5 kV, i_C = 1.5 kA, $L_{\sigma 1}$ = 120 nH and GU-1).

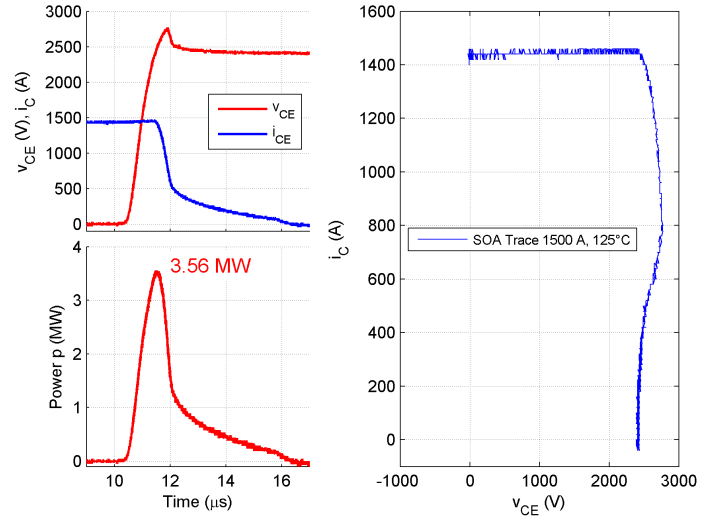

Fig. 31: IGBT turn-off waveforms, power and SOAR (Tj = 125 °C, V_{DC} = 2.5 kV, i_C = 1.5 kA, $L_{\sigma 1}$ = 120 nH and GU-1).

V. Conclusions

The new Westcode press pack SPT+ IGBT combines the advantages of the SPT+ technology with that of press-pack cases. The content of this paper is a detailed characterization of the new 85 mm, 4.5 kV, 1.2 kA Westcode press-pack SPT+ IGBT at hard switching.

Both IGBT and the corresponding freewheeling diode are characterized at hard turn-on and turn-off transients in all relevant operating conditions.

A variation of gate resistances in a range of $R_{G,on}$ = 3.3 to 6.8 Ω substantially influences the IGBT turn-on and the diode turn-off transients modifying voltage and current slopes, peak reverse recovery currents and switching losses. In contrast, an adjustment of the gate resistance $R_{G,off}$ in a range between 2.2 and 6.8 Ω does not substantially influence the IGBT turn-off behavior. The investigation of different stray inductances showed, that an increase of the stray inductance from $L_{\sigma 1} = 120$ nH to $L_{\sigma 2} = 210$ nH increases the overvoltages of IGBT and diode turn off transients at nominal i_C current and 2.5 kV dc-link voltage by about 130 V and 480 V respectively ($v_{CE} = 2.82$ kV to 2.95 kV, $V_D = 2.31$ kV to 2.89 kV). The increase of the stray inductance decreases the total switching losses of IGBT and diode. The switching losses as a function of dc-link voltage, load current, junction temperature and gate unit conditions are considered in detail. Assuming a dc-link voltage of 2.5 kV, a junction temperature of Tj = 125 °C and the minimum recommended gate resistances of $R_{G,on}$ and $R_{G,off}$ (GU-1), switching losses of about $E_{on,IGBT}$ 3.15 mJ/A at 25 °C and 3.34 mJ/A at 125 °C, $E_{off,IGBT}$ 3.58 mJ/A at 25 °C and 4.23 mJ/A at 125 °C, $E_{off,Diode}$ 1.47 mJ/A at 25 °C and 2.78 mJ/A at 125 °C are generated. Summarizing, the results show that the 4.5 kV, 1.2 kA Westcode press-pack SPT+ IGBT is an interesting power semiconductor for medium voltage converters.

References

[1] S. Bernet, "State of the art and developments of medium voltage converters an overview," in *Proc. PELINCEC 2005*, Warsaw, Poland, 2005.

[2] J. Rodriguez, S. Bernet, B. Wu, J. Pontt, and S. Kouro, "Multilevel voltage-source-converter topologies for industrial medium-voltage drives," *IEEE Trans. on Industrial Electron.*, vol. 54, no. 6, pp. 2930–2945, Dec. 2007.

[3] S. Bernet, "Recent developments of high power converters for industry and traction applications," *IEEE Trans. on Power Electron.*, vol. 15, no. 6, pp. 1102–1117, Nov 2000.

[4] F. Wakeman and G. Lockwood, "Electromechanical evaluation of a bondless pressure contact igbt," *IEE Proceedings Circuits, Devices and Systems*, vol. 148, no. 2, pp. 89–93, Apr 2001.

[5] S. Bernet, "State-of-the-art and trends of high voltage power devices and medium voltage converters for industry and transportation," in *Proc. 5th International Workshop: Future of Electronic Power Processing and Conversion, IEEE-FEPPCON*, Salina, Italy, 2004.

[6] K. Fujii, P. Koellensperger, and R. De Doncker, "Characterization and comparison of high blocking voltage IGBTs and IEGTs under hard- and soft-switching conditions," *IEEE Trans. on Power Electron.*, vol. 23, no. 1, pp. 172–179, Jan. 2008.

[7] D. Linzen, J. von Bloh, and R. De Doncker, "Characterization of a high-voltage press pack IGBT under soft-switching conditions," *Conf. Rec. IEEE-IAS Annu. Meeting*, vol. 3, pp. 2170–2174 vol.3, 2002.

[8] M. Rahimo, A. Kopta, S. Eicher, U. Schlapbach, and S. Linder, "Switching-self-clamping-mode "SSCM", a breakthrough in SOA performance for high voltage IGBTs and diodes," in *Proc. Int. Symp. on Power Semiconductor Devices and ICs, ISPSD*, Kitakyushu, Japan, May 2004.

[9] M. Rahimo, A. Kopta, R. Schnell, U. Schlapbach, S. Zehringer, and S. Linder, "2.5kv-6.5kv industry standard IGBT modules setting a new benchmark in SOA capability," in *Proc. 25th International PCIM Conference*, Nuernberg, Germany, May 2004, pp. 314–319.

[10] S. Tschirley and S. Bernet, "Automated testing of high power semiconductor devices," in *Proc. of International Conference on Power Electronics and Intelligent Control for Energy Conservation*, Warsaw, Poland, 2005.